4-Amino-2-trifluoromethyl-phenyl retinate inhibits the migration of BGC-823 human gastric cancer cells by downregulating the phosphorylation level of MLC II

ANLA HU[1-3], YANYAN YANG[2], SUMEI ZHANG[2], QING ZHOU[2], WEI WEI[1] and YUAN WANG[1,2]

[1]Institute of Clinical Pharmacology, Anhui Medical University; [2]Laboratory of Molecular Biology and Department of Biochemistry, Key Laboratory of Anti-Inflammatory and Immunological Pharmacology, Ministry of Education and Key Laboratory of Gene Resource Utilization for Severe Disease of Anhui Province, Anhui Medical University, Hefei, Anhui 230032; [3]Department of Food and Nutrition Hygiene, School of Public Health, Anhui Medical University, Hefei, Anhui 230601, P.R. China

Received March 27, 2014; Accepted June 24, 2014

DOI: 10.3892/or.2014.3343

Abstract. 4-Amino-2-trifluoromethyl-phenyl retinate (ATPR) is a novel all-trans retinoic acid (ATRA) derivative which was reported to have a superior antitumor effect in breast cancer cells. However, little is known about its antitumor effects on human gastric cancer cells and the mechanisms have not been fully elucidated. The results of the present study suggest that in the human gastric carcinoma cell line BGC-823, ATPR plays a more effective role than ATRA at the same dose in inhibiting proliferation, migration and inducing differentiation after the same treatment time. Furthermore, we investigated the preliminary mechanism of ATPR's anti-migration effect. Immunofluorescence assay demonstrated that claudin-18 positioned from cytoplasm to cell surface following ATPR stimuli. Real-time quantitative RT-PCR and western blot analyses showed that ATPR had significant effects on downregulation of the phosphorylation level of myosin light chain II (MLC II) by suppressing myosin light chain kinase (MLCK) and Rho-associated coiled-coil containing kinase (ROCK), as well as its regulation in the protein expression of RARα and RARβ. Moreover, ATPR increased the activity of myosin phosphatase by inhibiting ROCK. Consequently, ATPR showed more promising antitumor effects than ATRA in BGC-823 *in vitro*, and it may conduct its anti-migration effects by decreasing the phosphorylation level of MLC II, as well as by regulating MLCK and ROCK as downstream target genes.

Correspondence to: Professor Yuan Wang, Laboratory of Molecular Biology and Department of Biochemistry, Key Laboratory of Anti-Inflammatory and Immunological Pharmacology, Ministry of Education and Key Laboratory of Gene Resource Utilization for Severe Disease of Anhui Province, Anhui Medical University, Hefei, Anhui 230032, P.R. China
E-mail: wangyuan@ahmu.edu.cn

Key words: ATPR, gastric cancer, migration, p-MLC II, MLCK, ROCK

Introduction

Gastric cancer is the second most common cause of cancer-related mortality with little improvement in long-term survival during the past decades (1). Chemotherapy constitutes an important treatment regimen for gastric cancer in addition to surgical resection. However, in clinical application, there are still no recognized standards on chemotherapy regimens (2). Thus, novel agents that are non-toxic, efficacious as new recognized standards are urgently required.

All-trans retinoic acid (ATRA) is one of the vitamin A metabolites. Since FDA approved ATRA for treating acute promyelocytic leukemia in 1995, ATRA has been widely studied in cancer since it plays important roles in cell differentiation, growth and apoptosis (3). However, the extensive use of ATRA in oncology is hampered by both the toxicity and the development of ATRA resistance during chemotherapy (4). Thus, there is a constant need to find more effective and low-poisonous derivatives of ATRA. 4-Amino-2-trifluoromethyl-phenyl retinate (ATPR) is a novel ATRA derivative which was designed and synthesized by our team (5). The superior antitumor effects of ATPR compared to ATRA have been demonstrated on a human breast cancer cell line in our previous studies (6). In the present study, we compared the effects of ATPR and ATRA on proliferation, differentiation and migration of human gastric carcinoma cell line BGC-823 *in vitro*. BGC-823 is a poorly-differentiated human gastric adenocarcinoma cell line with fast-proliferation and high-malignant characteristics, commonly used in China and also adopted in the UK, Germany, Italy and Russia (7).

Similar to other solid human cancers, recurrence and metastasis are the biggest obstacles in the treatment of gastric cancer. Cell migration is critical for a variety of biological processes in normal and pathological conditions including cancer metastasis (8). In cell migration, a contractile force drives the cell body forward, and the rear part of the cell is detached from the substrate. Myosin II is believed to be involved in the generation of the contractile force for cell migration. The activity of myosin II is mainly controlled by myosin

light chain (MLC II) phosphorylation, which is considered to promote myosin assembly and increase the actomyosin-based contractility (9). Furthermore, the phosphorylation of MLC II is regulated by some enzymes. Myosin light chain kinase (MLCK) and Rho-associated coiled-coil containing kinase (ROCK) are two major enzymes that phosphorylate MLC II; however, myosin phosphatase (MLCP) plays opposite roles in MLC II phosphorylation (10). MLCP is a trimeric complex consisting of a regulatory myosin-binding subunit (MYPT1), a catalytic subunit, and a subunit of unknown function. MLCP drives the dephosphorylation of MLC II, which becomes inactive when MYPT1 is phosphorylated (11). In particular, ROCK can not only directly phosphorylate MLC II, but it can also increase the phosphorylation level of MLC II indirectly by phosphorylating MYPT1, thus inhibiting its phosphatase activity (12). Based on these findings, in the present study we surveyed whether ATPR can inhibit the migration of BGC-823 cells *in vitro*, and observed whether ATPR affects the position of claudin-18, one of the tight junction proteins, and identified whether ATPR play its anti-migration roles by suppressing the expression of MLCK and ROCK.

It is well known that ATRA plays its roles by activating retinoic acid receptors (RARs) that bind to retinoid X receptors (RXRs) as a heterodimer, and then this heterodimer binds to a regulatory DNA element (retinoic acid response elements; RAREs) and regulates the transcriptional expression of downstream target genes (13). However, whether ATPR works by activating RARs and its downstream genes is not very clear. In the present study, we used the BGC-823 cell line, which is a RARα and RARβ-positive cell line (14), and identified whether ATPR affects the expression of RARα and RARβ by targeting MLCK and ROCK as downstream genes.

Materials and methods

Cell lines and major reagents. The human poorly-differentiated gastric carcinoma cell line BGC-823 was obtained from the Cell Bank at the Chinese Academy of Science (Shanghai, China). Cells were cultured in RPMI-1640 medium (Gibco, USA) supplemented with 10% fetal bovine serum (Tianhang, China), 100 U/ml penicillin and 100 μg/ml streptomycin at 37˚C in a humidified atmosphere containing 5% CO_2.

ATPR was synthesized by the School of Pharmacy, Anhui Medical University, and was dissolved in dimethyl sulfoxide (DMSO) at the stock concentration of 10 mmol/l and stored at -20˚C. ATRA, MTT and DMSO were purchased from Sigma-Aldrich (USA). Primary antibodies, including anti-RARα (C-20) (sc-551), anti-RARβ (C-19) (sc-552), anti-MLCK (L-18) (sc-9452), anti-p-MLC II (Thr18/Ser19) (sc-12896), anti-MLC II (D-9) (sc-48414), anti-p-MYPT1 (Thr853) (sc-17432), anti-MYPT1 (H-130) (sc-25618), anti-claudin-18 (P-14) (sc-17687) and anti-β-actin (C4) (sc-47778) were purchased from Santa Cruz Biotechnology (USA). All secondary antibodies were purchased from Millipore (USA).

MTT assay. Cell proliferation after ATPR administration was estimated by the MTT assay. The BGC-823 cells were plated on 96-well cell culture plates at a density of $4x10^3$ cells/well. After incubation for 24 h, ATPR was added to the wells at gradual concentrations of 5, 10, 15, 20, 30 and 40 μmol/l, and then incubated in a humidified incubator at 37˚C with 5% CO_2. The cells treated with 40 μmol/l ATRA were taken as the positive control and the cells treated with 0.1% DMSO were the solvent control. After a 48-h incubation period, the medium was removed and 5 mg/ml MTT solution was added to each well. Cells were incubated for 4 h, followed by the addition of 100 μl DMSO and the mixture was incubated for 10 min to dissolve formazan crystals. The absorbance was measured at a wavelength of 570 nm using a microplate reader (BioTek Model ELx800). Inhibition rate (%) was calculated according to the following formula: (1-OD_{570} of drug/OD_{570} of control) x 100%.

Plate colony formation assay. The colony formation ability of BGC-823 cells *in vitro* was measured by plate colony formation assay. BGC-823 cells in the exponential phase of growth were exposed to ATPR for 48 h, and then harvested as single cell suspensions. Approximately 1,000 cells were added to each well of a 6-well cell culture plate. The plate was incubated for 8-10 days in a humidified atmosphere at 37˚C until the colonies were clearly visible to the naked eye. We removed the medium from each well, gently washed each well by phosphate-buffered saline (PBS) two times, fixed the cells by 4% paraform and stained with 1% crystal violet. The colonies containing >50 cells were counted in each well for five random visual fields. The mean colony count for each of the treatments was calculated.

Flow cytometry. Detection of cell cycle was performed by PI stained flow cytometry. BGC-823 cells in the exponential phase of growth were exposed to ATPR for 48 h, then harvested as single cell suspensions, washed with cold PBS two times and then tested by Coulter DNA-Prep Reagents kit (Beckman Coulter, USA) according to the manufacturer's manual. Cell cycle distribution was analyzed by FACSCalibur flow cytometry (Becton-Dickinson).

Colorimetric detection of the activities of alkaline phosphatase (ALP) and lactate dehydrogenase (LDH). ALP and LDH activities of BGC-823 cells treated with ATPR for 48 h were assayed. The cells were collected, washed with PBS, and then lysed with 0.2% Triton-X 100 for 30 min on ice. The cell lysate was centrifuged at 14,000 rpm at 4˚C for 15 min. The ALP and LDH activities in the supernatant were measured by the colorimetric method using Olympus AU400. The total protein concentration in the supernatant was determined by BCA assay. The enzyme activity was expressed as activity/total protein (U/g).

Wound healing assay. The migration ability of BGC-823 cells was measured by the wound healing assay. BGC-823 cells were cultured in a 24-well cell culture cluster to form a monolayer that was >90% confluent. Then, the cell monolayer was scraped with a sterile pipette tip to generate the wound. Thereafter, the cells were washed with RPMI-1640 medium and then re-cultured in fresh medium with ATPR or ATRA for 48 h. Images were captured at 0, 24 and 48 h on the same position of the wound with an inverted phase contrast microscope (Leica DMI3000 B). The width of the wound was measured with Quantity One software.

Immunofluorescence assay. The position of claudin-18 was observed by immunofluorescence assay. BGC-823 cells were seeded at a density of $1x10^4$ cells/ml into a 6-well cell culture cluster with sterile coverslips and cultured. When cells grew in form of monolayer, cells were treated with 25 μmol/l ATPR or ATRA for 72 h, and cells treated with 0.1% DMSO were used as a control group. After treatment, the cells were washed with PBS 3 times and fixed with 4% paraformaldehyde for 20 min at room temperature, then washed and blocked with blocking buffer (PBS/5% non-fat dry milk) for 2 h at room temperature. The coverslips with cells were incubated with goat anti-human claudin-18 (1:50) primary antibody overnight at 4˚C. Subsequently, the coverslips were washed and incubated with donkey anti-goat IgG-FITC (1:100) for 2 h at room temperature away from light, then washed and incubated with DAPI for 5 min, and then washed and mounted with aqueous-based anti-fade mounting medium, finally fixed with colorless nail polish on microscope slides. Images of stained cells were captured by fluorescence microscope (Leica DMI4000 B).

Real-time quantitative PCR (qRT-PCR). qRT-PCR was performed to quantify the mRNA levels of MLCK, ROCK1 and ROCK2. Total cellular RNA was isolated from cultured cells by TRIzol solution (Invitrogen, USA), and 1 μg of total RNA was reverse-transcribed by PrimeScript™ RT reagent kit with gDNA Eraser (Takara, China) according to the manufacturer's protocol. The complementary DNAs were amplified by UltraSYBR Mixture (CWBiotech, China) by using a Real-Time PCR System (Thermo, USA) with the following primer sets: MLCK, 5'-ggactttcagccttgtgattc-3' (forward) and 5'-cgcaaaacttccttctactgtc-3' (reverse); ROCK1, 5'-ctctaccactttcctgccaa-3' (forward) and 5'-gtggcacttaacatggcatc-3' (reverse); ROCK2, 5'-accaatgctttactgcgaac-3' (forward) and 5'-tctccagcaggcagttttta-3' (reverse); 18S rRNA, 5'-cagccacccgagattgagca-3' (forward) and 5'-tagtagcgacgggcggtgtg-3' (reverse). All primers were synthesized by Sangon Biotech (China). 18S rRNA served as a reference gene. The PCR program was: template denaturation at 95˚C for 10 min; 40 cycles of template denaturation at 95˚C for 10 sec, primer annealing at 56˚C for 30 sec, product extension at 72˚C for 32 sec; a final PCR product extension at 60˚C for 30 sec. Results are shown by the mean normalized values of cDNA levels among each group with the reference gene.

Western blot analysis. To determine the changes of protein levels, the cellular total protein of BGC-823 was extracted after different treatment. At specific time points, cells were washed with PBS 3 times and protein extracts were prepared with RIPA buffer and quantified by BCA protein assay (Beyotime, China). Thirty micrograms of protein were resolved in SDS sample buffer, fractionated in SDS-PAGE gels and transferred to a PVDF membrane. The membranes were blocked for 1 h at room temperature with TBST containing 5% non-fat dry milk and then incubated with the primary antibodies for RARα (1:500), RARβ (1:500), MLCK (1:500), p-MLC II (1:250), MLC II (1:500), p-MYPT1 (1:500), MYPT1 (1:700) and β-actin (1:1,000) overnight at 4˚C. The reactive bands were visualized with enhanced chemiluminescence (Beyotime).

Table I. The dose-effect of ATPR on BGC-823 cell proliferation.

Group	Concentration (μmol/l)	OD_{570} (mean ± SD)	Inhibition rate (%)
Cell		0.758±0.020	
DMSO-treated		0.745±0.010	
ATRA-treated	40	0.429±0.007	42.4±0.93
ATPR-treated	5	0.741±0.007	0.64±0.08
	10	0.732±0.016	1.78±0.02
	15	0.540±0.075	27.61±1.00
	20	0.466±0.083	37.5±1.12
	30	0.297±0.031	60.15±4.1
	40	0.289±0.015	61.19±2.0[a]

[a]Compared with ATRA-treated cells, P<0.01. ATPR, 4-amino-2-trifluoromethyl-phenyl retinate; ATRA, all-trans retinoic acid.

Statistical analysis. All experiments were repeated a minimum of 3 times. Data presented in images are from one representative experiment. Statistical significance was determined with one-way ANOVA with SPSS 17.0 software. A value of P<0.05 was considered to indicate a statistically significant difference.

Results

ATPR inhibits the proliferation of BGC-823 cells. To test the proliferation inhibitory effect of ATPR on BGC-823 cells, we performed an MTT assay and a plate colony formation assay. As shown in Table I, the proliferation ability of BGC-823 cells was significantly decreased in the treatment group compared to the solvent group. For the 40 μmol/l ATPR-treated cells, the OD 570 nm value was 0.289±0.015 while the value of the ATRA group was 0.429±0.007 at the same concentration (P<0.01). The results also showed that the proliferation of BGC-823 cells was inhibited by ATPR in a concentration-dependent manner. According to the above data, the IC_{50} value of ATPR was 27.86 μmol/l. Finally, 25 μmol/l was chosen as the treatment concentration for most of the following assays.

On the other hand, the colony formation ability of BGC-823 cells *in vitro* was determined by plate colony formation assay. BGC-823 cells treated with 25 μmol/l ATPR or 25 μmol/l ATRA were taken as the treatment groups and cells treated with 0.1% DMSO as the control group. After 8-10 days, we captured the images and statistically accounted the mean numbers of colonies. Fig. 1 shows that the colony formation ability of BGC-823 cells in the treatment groups was markedly reduced compared to the control group (P<0.01). Furthermore the mean numbers of colonies in the ATPR-treated group were lower than in the ATRA-treated group (P<0.01).

ATPR induces the differentiation of BGC-823 cells. To investigate the effect of ATPR on differentiation of BGC-823 cells, we observed the cell morphological changes, the cell cycle distribution and the activities of ALP and LDH. These results suggested that BGC-823 cells not only undergo differentiation

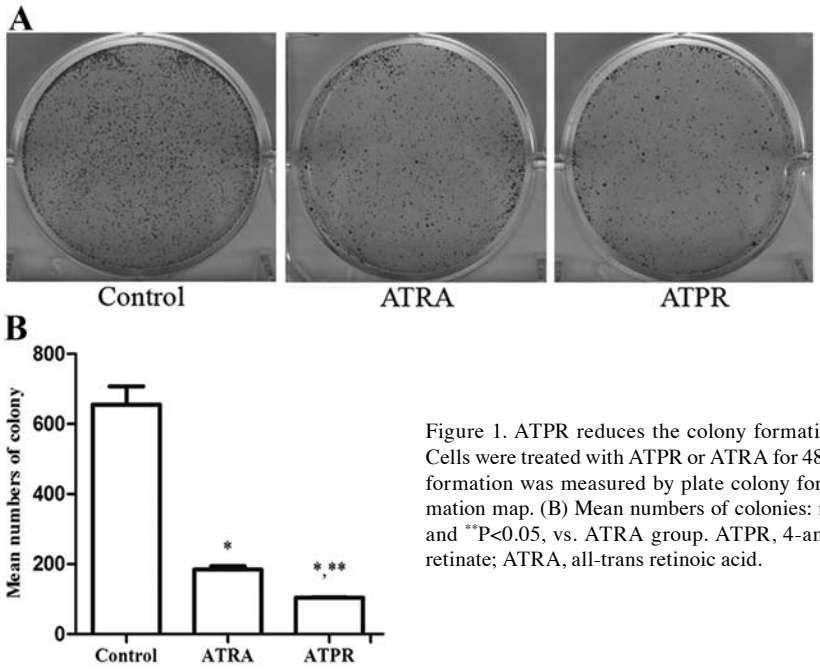

Figure 1. ATPR reduces the colony formation of BGC-823 cells *in vitro*. Cells were treated with ATPR or ATRA for 48 h and the ability of cell colony formation was measured by plate colony formation assay. (A) Colony formation map. (B) Mean numbers of colonies: n=3, *P<0.01, vs. control group and **P<0.05, vs. ATRA group. ATPR, 4-amino-2-trifluoromethyl-phenyl retinate; ATRA, all-trans retinoic acid.

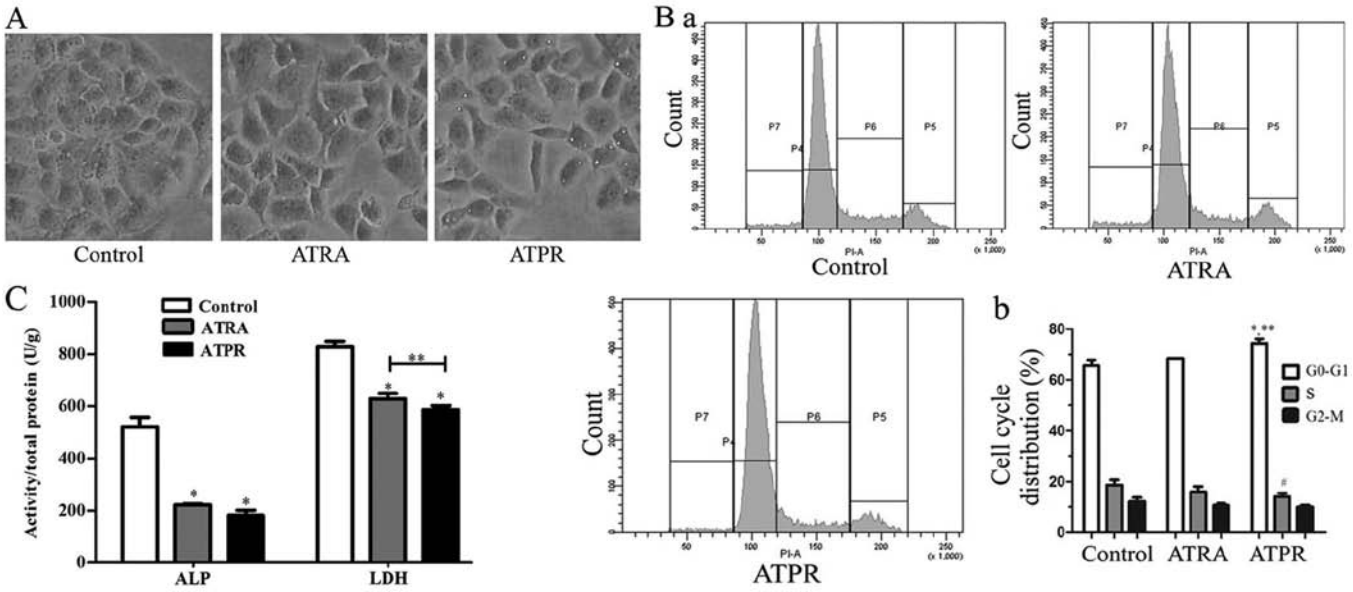

Figure 2. ATPR induces the differentiation of BGC-823 cells. BGC-823 cells were treated with ATPR or ATRA for 48 h. (A) ATPR-treated BGC-823 cells showed morphological changes characteristic of differentiating cells. Cell morphological changes were observed with an inverted phase contrast microscope. (B) ATPR-induced cell cycle significantly arrested at G_0-G_1 phase in BGC-823 cells. Cell cycles were determined by PI staining and quantified by FACS analysis. (B-a) Cell cycle map: P4, G_0-G_1 phase; P6, S phase; P5, G_2-M phase. (B-b) The distribution of cell cycle: n=3, *P<0.01 vs. control group; **P<0.01 vs. ATRA group and $^{\#}$P<0.05 vs. control group. (C) ATPR reduced the activities of ALP and LDH in BGC-823 cells. n=3, *P<0.01 vs. control group and **P<0.05 vs. ATRA group. ATPR, 4-amino-2-trifluoromethyl-phenyl retinate; ATRA, all-trans retinoic acid.

following ATPR treatment, but also that ATPR is more efficient than ATRA in inducing the differentiation of BGC-823 cells.

After the BGC-823 cells were treated with 25 μmol/l ATPR for 48 h, we observed the cell morphological changes with an inverted phase contrast microscope. ATPR-treated cells showed morphological changes with characteristics of differentiating cells, such as elongation or stretching of the cells as shown in Fig. 2A. ATPR induced more obvious changes in cell morphology than ATRA-treated cells at the same concentration. However, the control cells appeared hexagonal.

A cell cycle analysis of BGC-823 cells after treatment with 25 μmol/l ATPR for 48 h was performed by a flow cytometry. As shown in Fig. 2B, an accumulation of cells in G_0/G_1 phase with a reduction in the number of cells in S phase was observed. For the 0.1% DMSO-treated cells (the control group), 65.55±2.35 and 18.6±2.1% cells were detected in G_0/G_1 and S phases, respectively. For the cells treated with 25 μmol/l

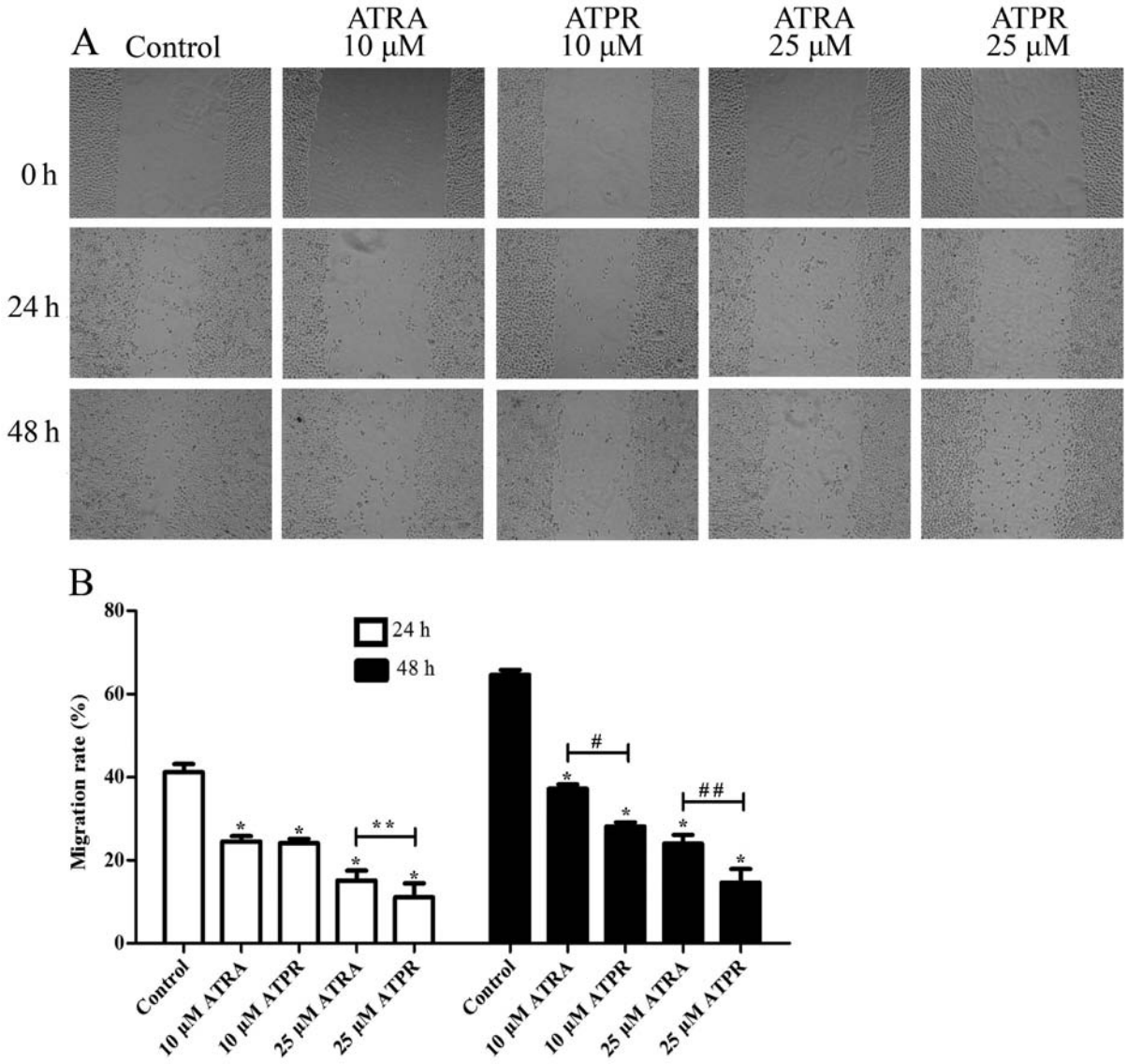

Figure 3. ATPR inhibits the migration of BGC-823 cells *in vitro*. Cell migration ability was detected by wound healing assay after BGC-823 cells were exposed to ATPR or ATRA for 48 h. (A) Migration map. (B) Analysis of migration rate: n=6, 24 h: *P<0.01 vs. control group and **P<0.05 vs. ATRA (25 μmol/l) group; 48 h: *P<0.01 vs. control group, $^{\#}$P<0.01, vs. ATRA (10 μmol/l) group and $^{\#\#}$P<0.01 vs. ATRA (25 μmol/l) group. ATPR, 4-amino-2-trifluoromethyl-phenyl retinate; ATRA, all-trans retinoic acid.

ATPR, 74.35±1.75 and 14.05±1.35% were detected in G_0/G_1 and S phases, respectively. The differences of G_0/G_1 phase (P<0.01) and S phase (P<0.05) between the control and ATPR-treated cells were statistically significant. However, there was no statistically significant difference between the control and the ATRA-treated cells. In addition, ATPR induced greater accumulation in G_0/G_1 phase than ATRA (P<0.01).

At the same time, we also detected the activities of ALP and LDH after ATPR treatment. The results (Fig. 2C) showed that the activities of ALP and LDH in ATPR-treated cells were lower than those in control cells. The activities of ALP and LDH in control cells were 522.17±35.69 and 828.75±19.67 U/g, respectively. In the cells treated with ATPR, the activities of ALP and LDH were 181.95±19.21 and 587.25±14.55 U/g, respectively. In the cells treated with ATRA, the activities of ALP and LDH were 221.90±4.40 and 628.72±21.10 U/g, respectively. The difference in the activity of the two enzymes between the control and treated cells was statistically significant (P<0.01). Moreover, ATPR suppressed the activity of LDH more than ATRA (P<0.05).

ATPR suppresses the migration of BGC-823 cells. To investigate the effect of ATPR on migration in BGC-823 cells, wound healing assay was performed. As shown in Fig. 3, wound healing assay illustrated that the migration rate of BGC-823 cells was inhibited by ATPR, and the effect reached statistical significance compared with the control group (P<0.01). Furthermore, ATPR had a significant effect on the migration of cells compared to ATRA at the same concentration. After culturing for 24 h, the migration rate of the 25 μmol/l ATPR group was 11.08±3.35% while that of the ATRA group was 15.12±2.40% (P<0.05). After culturing for 48 h, the migration rate of the 10 μmol/l ATPR group was 28.08±0.99% while that of the ATRA group was 37.16±1.09% (P<0.01).

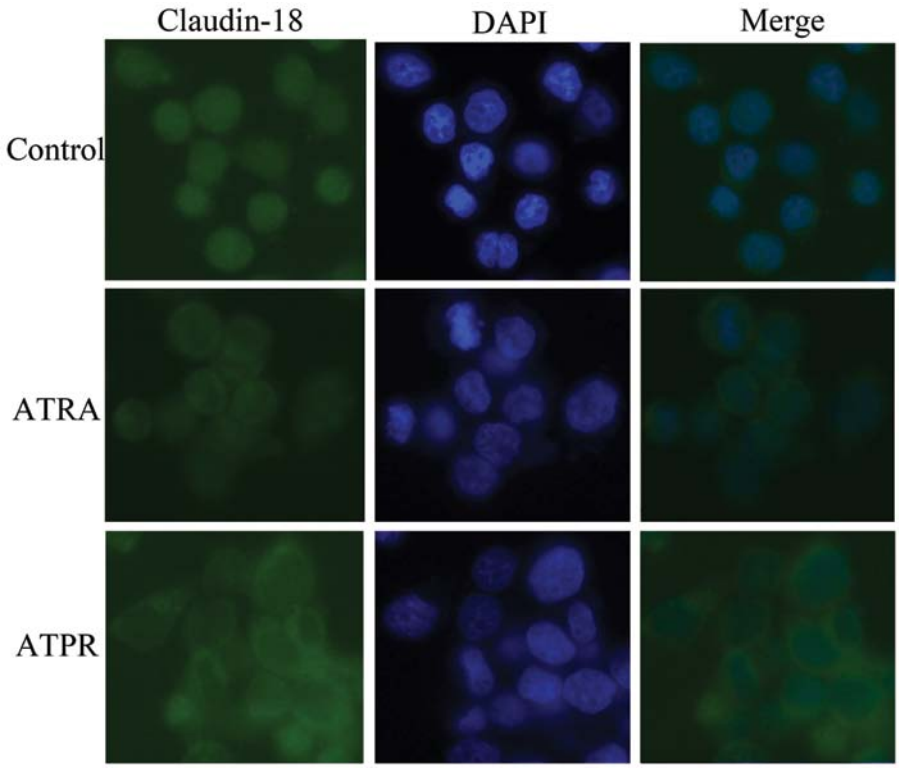

Figure 4. ATPR changes the cellular localization of claudin-18 in BGC-823 cells. After BGC-823 cells were treated with ATPR or ATRA for 72 h, nuclei were counterstained with DAPI (blue). Immunofluorescence microscopy showed that claudin-18 labeled with green fluorescent protein accumulated on the cell surface in the ATPR-treated group while in the control group, claudin-18 positioned on the cytoplasm. ATPR, 4-amino-2-trifluoromethyl-phenyl retinate; ATRA, all-trans retinoic acid.

ATPR changes the localization of claudin-18 in BGC-823 cells. As shown in Fig. 4, immunofluorescence assay displayed that, in the control group, claudin-18 labeled with green fluorescent protein positioned at the cytoplasm well-distributed, while in the treatment groups, claudin-18 mainly concentrated on the cell surface. Moreover, in the ATPR group, claudin-18 accumulation was clearly increased compared to the ATRA group.

ATPR reduces the protein expression of RARα and RARβ in BGC-823 cells. Fig. 5A shows that the protein expression levels of RARα and RARβ after treatment with drugs were all decreased compared with the DMSO control group ($P<0.05$). However, the protein expression levels in the ATPR group decreased more than in the ATRA group, particularly in the protein expression of RARβ ($P<0.01$).

ATPR suppresses MLCK and ROCK at transcriptional and translational levels in BGC-823 cells. In order to investigate whether MLCK and ROCK play a potential role in the anti-migration effects of ATPR, qRT-PCR and western blotting were applied to analyze the mRNA and protein changes of the MLCK and ROCK after treatment with ATPR. Two days after treatment, we harvested cells for RNA isolation. As shown in Fig. 5B, the mRNA levels of MLCK ($P<0.05$), ROCK1 ($P<0.01$) and ROCK2 ($P<0.01$) were significantly downregulated in the ATPR group compared to the control group. Although the mRNA levels in the ATPR group decreased more than in the ATRA group, there was no statistical significance between the two groups.

Western blot analysis, shown in Fig. 5C, revealed that in the treatment groups, the protein expression of MLCK, the phosphorylation levels of MLC II and MYPT1 were decreased compared with the control group ($P<0.05$). In addition, ATPR showed greater effects than ATRA on the phosphorylation status of MLC II and MYPT1 ($P<0.05$).

Discussion

In the present study, we investigated the antitumor effects of ATPR, a novel ATRA derivative, in human gastric cancer cell line BGC-823, and explored the initial mechanism involved in the anti-migration effect. Our results demonstrated that ATPR has a promising inhibitory effect compared to ATRA on BGC-823 *in vitro*. MTT assay and plate colony formation assay demonstrated that ATPR inhibits the proliferation ability of BGC-823 cells. Cell cycle analysis, detection of the activities of alkaline phosphatase (ALP) and lactate dehydrogenase (LDH) combined cell morphological changes indicated that ATPR clearly induces the differentiation in BGC-823 cells. Wound healing assay showed that ATPR suppresses the migration activity of BGC-823 cells *in vitro*, and immunofluorescence assay revealed that claudin-18 translocates from the cytoplasm to the cell surface after ATPR treatment. To explore the preliminary mechanism, we performed real-time quantitative RT-PCR and western blot analyses, and then found that ATPR decreases the expression of MLCK and ROCK in BGC-823 cells at transcriptional and translational levels.

ATPR is one of the ATRA derivatives designed and synthesized by our team (5). It is well-known that ATRA is

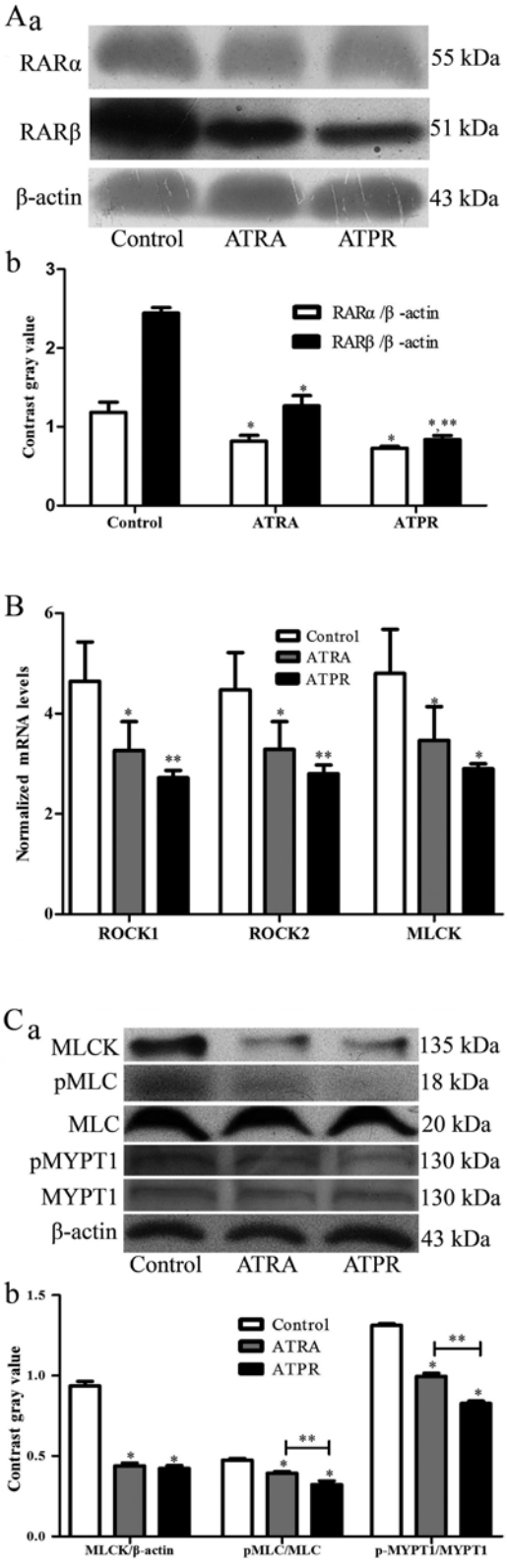

Figure 5. Possible mechanism of ATPR inhibition of the migration of BGC-823 cells. Cells were treated with 25 μmol/l ATPR or ATRA for 48 h. (A-a) Western blot analyses revealed that ATPR reduced the protein expression levels of RARα and RARβ. (A-b) Analysis of contrast gray value: n=3, *P<0.01 vs. control group and **P<0.01 vs. ATRA group. (B) ATPR downregulated the mRNA levels of ROCK1, ROCK2 and MLCK of BGC-823 cells detected by qRT-PCR. n=3, *P<0.05 vs. control group; **P<0.01 vs. control group. (C-a) The expressions of MLCK, p-MLC and p-MYPT1 were analyzed using western blotting. β-actin, MLC and MYPT1 were respectively used as loading control. (C-b) Analysis of contrast gray value: n=3, *P<0.05 vs. control group; **P<0.05 vs. ATRA group. ATPR, 4-amino-2-trifluoromethyl-phenyl retinate; ATRA, all-trans retinoic acid.

a classical differentiation agent. Nevertheless, in the present study, ATPR exhibited superior differentiation-inducing activity compared to ATRA on human gastric cancer cell line BGC-823. Several studies have shown that ATRA-induced differentiation is tightly coupled to growth arrest in the G_0/G_1 phase, which usually represents the cell differentiation (7,15). The present study also demonstrated the coincidental result that stimulation under ATRA or ATPR arrested the cell cycle of BGC-823 cells in G_0/G_1 phase. In addition, the accumulation effect of ATPR was stronger than that of ATRA. ALP and LDH are two enzymes known for their involvement in the differentiation of gastric cells. The activities of these two enzymes are both upregulated in gastric cancer; however, both enzymes are decreased in the process of normal gastric cell differentiation, indicating that the enzymes function as dedifferentiation factors in the stomach (16,17). In the present study, we found that the activities of ALP and LDH in BGC-823 cells were markedly decreased by ATPR. The activities of the two enzymes were also reduced by ATRA, but the effect was weaker than by ATPR.

It is well established that inhibition of cancer cell growth by ATRA is mediated by retinoic acid receptors (RARs). Activated RARs regulate the expression of multiple target genes, including genes involved in differentiation, cell cycle control and migration, and thus often inhibit cell growth (13,18). The structure of ATPR is similar to ATRA. However, little is known about whether ATPR plays its role by binding RARs. In this study, we detected the expression of RARα and RARβ after exposure to ATPR, and the results of western blot analyses showed that the expression levels of RARα and RARβ were decreased, indicating that ATPR can influence the expression of RARs; however, further studies are required to confirm whether ATPR can bind to RARs.

Phosphorylation of MLC II is important for the activity of myosin which is responsible for actomyosin contractility and hence cell migration. Phosphorylation of MLC II is regulated mainly by two distinct signal transduction cascades. One pathway requires phosphorylation of MLC by MLCK, while the second pathway involves ROCK activation. It has been found that ML-7, a selective inhibitor of MLCK, could significantly inhibit the migration of breast cancer cell lines (19), and MLCK shows DNA hypermethylation in gastric cancer (20). The mRNA expression level of MLCK increases in non-small cell lung cancer and is associated with recurrence and metastasis (21). On the other hand, there is considerable evidence to suggest that ROCK becomes hyperactivity in many cancers, including gastric cancer, and contributes to more aggressive tumor properties such as metastasis and invasion (22-24). Two isoforms of ROCK have been described that are encoded by two separate genes, ROCK1 and ROCK2 (25). In the present study, real-time quantitative RT-PCR showed that the ATPR can reduce the mRNA levels of MLCK, ROCK1 and ROCK2. This means ATPR can affect MLCK and ROCK at the transcriptional level. Moreover, ATPR has an impact on MLCK and ROCK at the translational level for the data as western blot analyses revealed that the MLCK, p-MLC II and p-MYPT1 were downregulated by ATPR. The phosphorylation of MLC II and MYPT1 has been widely used as surrogate markers of ROCK activity. Since ROCK can phosphorylate MLC II directly and inhibit the dephosphorylation of MLC II

by phosphorylating the myosin-binding subunit (MYPT1) of MLCP, it can phosphorylate MLC II indirectly.

To a certain extent, we verified that ATPR inhibits the phosphorylation of MLC II in a MLCK- and ROCK-dependent manner, and then suppresses the cell migration. Although both MLCK and ROCK can phosphorylate MLC, Totsukawa *et al* hypothesized that MLCK would result in a high turnover rate of MLC phosphorylation while ROCK may achieve a slower phosphorylation of MLC (10). Although in this study we did not observe a clear distinction in ATPR on the role of suppressing these two kinases, the effect of ATPR on inhibiting the MLC phosphorylation may be different at different time points due to the active MLCP increased by inhibiting ROCK.

On the other hand, cytoskeletal contraction induced by phosphorylation of MLC can regulate tight junction barrier function and result in disruption of tight junction structure (26). Claudins are the major elements of tight junction complexes, such as occludins, JAMs and ZO-1 (27). Claudin-18 is mainly expressed in stomach and lung epithelial cells, and may be a good marker for gastric cancer (28,29). Oshima *et al* showed that downregulation of claudin-18 is related to the proliferative potential at the invasive front of gastric cancer (30). Our data showed that after ATPR stimuli, claudin-18 proteins positioned from cytoplasm to cell surface, which indicated that the translocation of claudin-18 to enhance the tight junction may be contributed to the anti-migration effect of ATPR.

According to the above results, ATPR can suppress the migration by influencing claudin-18, MLCK and ROCK, consequently inhibiting the proliferation and inducing the differentiation in BGC-823 cells. Our findings provide an experimental basis for the use of ATPR as chemotherapy drugs against gastric caner cells, thereby facilitating the development of new anticancer agents.

Acknowledgements

This study was supported by a National Nature Science Research Grant (no. 81272399).

References

1. Vogiatzi P, Vindigni C, Roviello F, Renieri A and Giordano A: Deciphering the underlying genetic and epigenetic events leading to gastric carcinogenesis. J Cell Physiol 211: 287-295, 2007.
2. Mackenzie M, Spithoff K and Jonker D: Systemic therapy for advanced gastric cancer: a clinical practice guideline. Curr Oncol 18: e202-e209, 2011.
3. Connolly RM, Nguyen NK and Sukumar S: Molecular pathways: current role and future directions of the retinoic acid pathway in cancer prevention and treatment. Clin Cancer Res 19: 1651-1659, 2013.
4. Garattini E, Gianni M and Terao M: Retinoids as differentiating agents in oncology: a network of interactions with intracellular pathways as the basis for rational therapeutic combinations. Curr Pharm Des 13: 1375-1400, 2007.
5. Gui SY, Chen FH, Zhou Q and Wang Y: Effects of novel all-trans retinoic acid retinamide derivatives on the proliferation and apoptosis of human lung adenocarcinoma cell line A549 cells. Yakugaku Zasshi 131: 1465-1472, 2011.
6. Wang B, Yan Y, Zhou J, Zhou Q, Gui S and Wang Y: A novel all-trans retinoid acid derivatives inhibits the migration of breast cancer cell lines MDA-MB-231 via myosin light chain kinase involving p38-MAPK pathway. Biomed Pharmacother 67: 357-362, 2013.
7. Zhang G, Wang G, Wang S, Li Q, Ouyang G and Peng X: Applying proteomic methodologies to analyze the effect of hexamethylene bisacetamide (HMBA) on proliferation and differentiation of human gastric carcinoma BGC-823 cells. Int J Biochem Cell Biol 36: 1613-1623, 2004.
8. Olson MF and Sahai E: The actin cytoskeleton in cancer cell motility. Clin Exp Metastasis 26: 273-287, 2009.
9. Somlyo AP and Somlyo AV: Signal transduction by G-proteins, rho-kinase and protein phosphatase to smooth muscle and non-muscle myosin II. J Physiol 522: 177-185, 2000.
10. Totsukawa G, Wu Y, Sasaki Y, *et al*: Distinct roles of MLCK and ROCK in the regulation of membrane protrusions and focal adhesion dynamics during cell migration of fibroblasts. J Cell Biol 164: 427-439, 2004.
11. Ito M, Nakano T, Erdodi F and Hartshorne DJ: Myosin phosphatase: structure, regulation and function. Mol Cell Biochem 259: 197-209, 2004.
12. Wong CC, Wong CM, Ko FC, *et al*: Deleted in liver cancer 1 (DLC1) negatively regulates Rho/ROCK/MLC pathway in hepatocellular carcinoma. PLoS One 3: e2779, 2008.
13. Soprano DR, Qin P and Soprano KJ: Retinoic acid receptors and cancers. Annu Rev Nutr 24: 201-221, 2004.
14. Wu Q, Chen ZM and Su WJ: Anticancer effect of retinoic acid via AP-1 activity repression is mediated by retinoic acid receptor α and β in gastric cancer cells. Int J Biochem Cell Biol 34: 1102-1114, 2002.
15. Fang Y, Zhou X, Lin M, *et al*: The ubiquitin-proteasome pathway plays essential roles in ATRA-induced leukemia cells G_0/G_1 phase arrest and transition into granulocytic differentiation. Cancer Biol Ther 10: 1157-1167, 2010.
16. Nowak G, Griffin JM and Schnellmann RG: Hypoxia and proliferation are primarily responsible for induction of lactate dehydrogenase activity in cultured cells. J Toxicol Environ Health 49: 439-452, 1996.
17. Fishman WH: Recent developments in alkaline phosphatase research. Clin Chem 38: 2484, 1992.
18. Lu J, Zhang F, Yuan Y, Ding C, Zhang L and Li Q: All-*trans* retinoic acid upregulates the expression of p53 via Axin and inhibits the proliferation of glioma cells. Oncol Rep 29: 2269-2274, 2013.
19. Zhou X, Liu Y, You J, Zhang H, Zhang X and Ye L: Myosin light-chain kinase contributes to the proliferation and migration of breast cancer cells through cross-talk with activated ERK1/2. Cancer Lett 270: 312-327, 2008.
20. Chen L, Su L, Li J, *et al*: Hypermethylated *FAM5C* and *MYLK* in serum as diagnosis and pre-warning markers for gastric cancer. Dis Markers 32: 195-202, 2012.
21. Minamiya Y, Nakagawa T, Saito H, *et al*: Increased expression of myosin light chain kinase mRNA is related to metastasis in non-small cell lung cancer. Tumour Biol 26: 153-157, 2005.
22. Lochhead PA, Wickman G, Mezna M and Olson MF: Activating ROCK1 somatic mutations in human cancer. Oncogene 29: 2591-2598, 2010.
23. Liu N, Bi F, Pan Y, *et al*: Reversal of the malignant phenotype of gastric cancer cells by inhibition of RhoA expression and activity. Clin Cancer Res 10: 6239-6247, 2004.
24. Matsuoka T, Yashiro M, Kato Y, Shinto O, Kashiwagi S and Hirakawa K: RhoA/ROCK signaling mediates plasticity of scirrhous gastric carcinoma motility. Clin Exp Metastasis 28: 627-636, 2011.
25. Nakagawa O, Fujisawa K, Ishizaki T, Saito Y, Nakao K and Narumiya S: ROCK-I and ROCK-II, two isoforms of Rho-associated coiled-coil forming protein serine/threonine kinase in mice. FEBS Lett 392: 189-193, 1996.
26. Vicente-Manzanares M, Ma X, Adelstein RS and Horwitz AR: Non-muscle myosin II takes centre stage in cell adhesion and migration. Nat Rev Mol Cell Biol 10: 778-790, 2009.
27. Runkle EA and Mu D: Tight junction proteins: from barrier to tumorigenesis. Cancer Lett 337: 41-48, 2013.
28. Sanada Y, Oue N, Mitani Y, Yoshida K, Nakayama H and Yasui W: Down-regulation of the claudin-18 gene, identified through serial analysis of gene expression data analysis, in gastric cancer with an intestinal phenotype. J Pathol 208: 633-642, 2006.
29. Iravani O, Tay BW, Chua PJ, Yip GW and Bay BH: Claudins and gastric carcinogenesis. Exp Biol Med 238: 344-349, 2013.
30. Oshima T, Shan J, Okugawa T, *et al*: Down-regulation of claudin-18 is associated with the proliferative and invasive potential of gastric cancer at the invasive front. PLoS One 8: e74757, 2013.